Motion and pinning of charged macroscopic defects in solid ^{4}He with 5% ^{3}He

A. I. Golov and L. P. Mezhov-Deglin

Institute of Solid-State Physics, Academy of Sciences of the USSR
(Submitted 26 February 1991; resubmitted 7 April 1991)
Zh. Eksp. Teor. Fiz. **101**, 545–556 (February 1992)

A study is made of quasi-periodic bursts of negative charge current superposed on a steady current in two-phase hcp–bcc samples of ^{4}He containing 5% ^{3}He. The bursts are observed in a bounded interval of electric fields and at temperatures below 1 K. The appearance and disappearance of these current bursts when the temperature or the applied field changes have a threshold character, which makes it possible to plot the boundaries of the existence region of the bursts in the space of temperature versus electric field. The data are interpreted in a model based on the motion of charged low angle grain boundaries.

1. INTRODUCTION

Experimental studies of the motion of charges in solid helium in a diode superposed on a steady current have sometimes revealed quasi-periodic current bursts, whose repetition, frequency, amplitude, and duration depend on the strength of the applied electric field and the temperature. In the papers by Dahm and co-workers[1,2] (see also the review of Dahm[3]) these bursts began to be detected after plastic deformation of crystals of bcc ^{3}He (for charges of both signs) and hcp ^{4}He (only for motion of positive charges).

The following model has been proposed[2] to explain this effect. The plastic flow of the sample relative to the fixed electrodes of the diode gives rise to low-angle boundaries (dislocation walls), which can trap charges and move toward the collector under the influence of an electric field. As it approaches the collector the charged boundary discharges and relaxes toward its original position, where it is again charged, and the cycle repeats.

The motion of charged dislocations has been observed in many materials. For example, in the plastic deformation of metals the entrainment of electrons by moving dislocations is accompanied by voltage pulses when the dislocation walls reach the surface of the sample.[4] The motion of charged low-angle boundaries in an applied electric field has been observed in alkali halide crystals.[5] The problem of the motion of dislocations under the influence of an external electric force in alkali halide crystals[5] and in the present experiment in solid helium are quite similar. The difference is that in alkali halide crystals the vacancies and dislocations are charged, while in liquid helium the defects can be charged only by trapping charges injected from an external source. Therefore the magnitude and sign of the trapped space charge in solid helium depend on many conditions (temperature, sign of the current flowing, strength of the electric field, charging time, etc.).

The trapping of charges by defects of a crystal lattice (dislocations) associated with plastic deformation or thermal cycling has been observed by various authors.[2,3,6,7] A study of recovery processes in deformed samples of hcp ^{4}He has shown that newly introduced dislocations are mobile, and that the activation energy of their motion is close to the energies of vacancy creation.[8] The introduction of ^{3}He impurity atoms in concentrations below 1% has only a slight effect on the mobility of newly introduced dislocations, but at concentrations of the order of 5% ^{3}He they slow them down considerably. It is natural to expect that the properties of charged defects in pure helium and in solid solutions will also be different.

Measurements of the mobility of charges in samples grown from a mixture of ^{4}He + 5% ^{3}He were reported in Ref. 9. In those studies we observed that at temperatures below a certain critical temperature the curves of the steady-state current as a function of time in two-phase bcc–hcp samples exhibited quasi-periodic bursts of negative current, which were absent in single-phase bcc or hcp samples (see the preliminary report[10]). In sufficiently strong fields the bursts were regular, and their behavior was basically similar to that described in Ref. 2. In weak fields, however, we observed interesting threshold effects in the onset of bursts associated with variations in the voltage or temperature. The experimental data can be interpreted in a model based on the motion of low-angle grain boundaries.[2] The threshold effects may be due to pinning of dislocations by ^{3}He impurity atoms.

2. PROCEDURE

The construction of the low-temperature apparatus and the techniques used to measure the current and velocity of the injected charges were described in a previous paper.[11] Two planar diodes were placed one above the other in solid helium in a cylindrical ampoule of inner diameter 8 mm. Each diode consisted of a β-active source (a titanium–tritium target on a molybdenum substrate) and a copper collector with dimensions of 6×16 mm^2. The source–collector gap was $L = 0.3$ mm. Positive and negative ions were created by the ionizing β radiation in a solid-helium layer of thickness ~ 10 μm adjacent to the source. The sign of the charges moving through the crystal from the source toward the collector depended on the polarity of the voltage U applied between the source and collector.

The collector currents were much smaller than the saturation currents of the ionizing sources (around 10^{-8} A), i.e., the current through the diode was space-charge limited. In this case, the presence of the space charge caused the electric field E to increase from the source to the collector, and the field near the collector exceeded the average value U/L by 40%.[11] However, for purposes of estimation we will assume that $E \approx U/L$.

The onset of a two-phase system and the motion of the bcc–hcp interface in the space between the diode plates can

 0038-5646/92/020289-07$05.00

be monitored by measuring the current through the diode. The transit time t^* of the charges across the source–collector gap was determined from the position of the peak on the $I(t)$ curve when the voltage was turned on abruptly. Since the charges of different signs in crystals of the bcc and hcp phases have different mobilities (in the bcc phase $\mu_- \gg \mu_+$, while in the hcp phase $\mu_- \ll \mu_+$),[10-12] two peaks arise on the $I(t)$ curve in a two-phase sample (Fig. 1), corresponding to the arrival times of the charged particles at the collector in each of the phases. The first (fast) peak corresponds to motion in the hcp phase and the second is the contribution of the bcc phase, for positive charges (as in Fig. 1), and vice-versa for negative charges. The steady-state current through the diode (for $t \gg t^*$) in the region of space-charge limited currents is proportional to the mobility:

$$I_\infty = 9\mu U^2 S/8L^3, \quad \mu = 0{,}8L^2/t^* U. \qquad (1)$$

Here μ is the mobility of the charges, and S is the area corresponding to the given phase. Therefore, from the mobility of the charges and the values of the steady-state currents one can estimate the area of the diode occupied by each of the phases [for Eq. (1) to be valid it is necessary that the fraction of the space charge trapped by defects in the crystal be small, as is the case at sufficiently high temperatures and voltages]. In an analogous way we have previously followed[12] the motion of the interface between the hcp and bcc phases during thermal cycling in pure ^{4}He.

Figure 2 shows the curves of the velocity $V_+(T)$ at $U = 300$ V in the hcp and bcc phases in the transition region. We note that although the relative heights of the signals from the different phases are different on cooling and heating (corresponding to different amounts of the bcc and hcp phases in the interelectrode space), the position of the peaks, i.e., the transit time t^* of the charges, depends only on the temperature. The values of the mobility $\mu_\pm(T)$ measured for each of the phases in the two-phase samples are in essential agreement with those obtained in single-phase hcp or bcc samples at similar molar volumes.

The cold finger was located below, and the filling capillary entered the ampoule from above. The samples of solid helium were grown at a constant pressure p from a mixture of ^{4}He + 5% ^{3}He, which was prepared by mixing measured volumes of gases of the isotopes at room temperature. The p–T phase diagram of ^{4}He + 5% ^{3}He has a wide coexistence region of the bcc and hcp phases in terms of temperature.[13] When a bcc sample was cooled at constant volume in an isolated ampoule (molar volume $V_m = 21.1$ cm^3/mole) to below the phase transition temperature, the hcp phase arose in the colder part of the ampoule (the molar volume of the hcp phase is about 0.2 cm^3/mole smaller than that of the bcc phase). Under equilibrium conditions the ratio of the volumes of the different phases in the ampoule is determined by the temperature T and initial molar volume of the bcc sample.

The presence of two adjacent diodes made it possible to monitor the position of the phases along the length of the ampoule. The bcc phase always occupied the upper part of the ampoule and the hcp phase, the lower part. Therefore, by growing and sealing off the initial sample of the bcc phase at various pressures p in the range 29–33 atm, on cooling we ultimately obtained a single-phase sample in one of the diodes and a two-phase sample in the other (either the lower was hcp and the upper bcc + hcp or the lower was bcc + hcp and the upper bcc).

Quasi-periodic current bursts of negative polarity were observed in both the upper and lower diodes, but only when they contained two-phase hcp–bcc samples.

3. EXPERIMENTAL RESULTS

The main observations of current oscillations in the motion of negative charges in the mixture ^{4}He + 5% ^{3}He were made on eight samples. In different samples the amplitude, repetition frequency, and other characteristics of the bursts were somewhat different. The reproducibility of the results on a single sample, especially at high voltages, was satisfactory (e.g., as will be seen from Fig. 7, the value of the lower

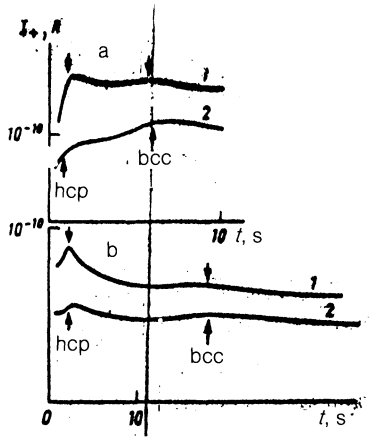

FIG. 1. Time dependence of the collector current $I(t)$ when a voltage $U = +300$ V is turned on abruptly at temperatures of 1.24 K (a) and 1.18 K (b), as measured in a two-phase bcc–hcp sample on heating (1) and cooling (2). The arrows indicate the times of arrival t^* of the charge fronts of the bcc and hcp phases.

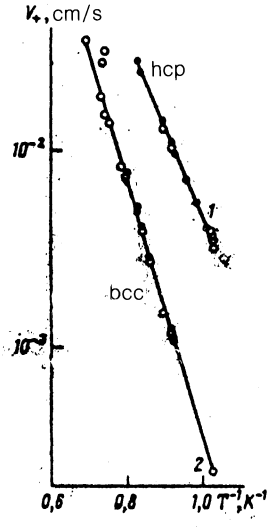

FIG. 2. Two plots of the temperature dependence of the velocity $V = L/t^*$ of positive charges at a voltage $U = +300$ V, as measured from the time of arrival of the two charge fronts on the $I(t)$ curves (as in Fig. 1) in a mixed bcc–hcp phase. Curve 1 (the first front) corresponds to the velocity of charges in the hcp phase, curve 2 (the second front) to that in the bcc phase; the measurements were made on heating (○) and cooling (●).

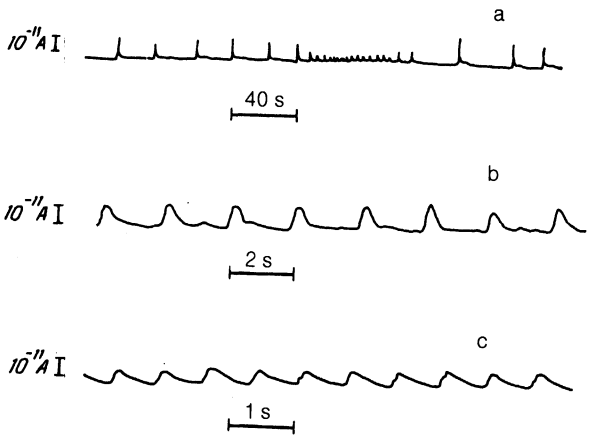

FIG. 3. Oscillations of the negative current in a diode at different values of the applied voltage and steady-state current: a) $U = 267$ V, $I_\infty = 1.24 \cdot 10^{-10}$ A; b) $U = 500$ V, $I_\infty = 6.0 \cdot 10^{-10}$ A; c) $U = 800$ V, $I_\infty = 1.26 \cdot 10^{-9}$ A. Sample No. 2, $T = 0.91$ K. The time and current scales are indicated on each diagram separately.

threshold field U_{lower} in sample No. 1 at $T = 1.00$ K, measured after a period of days, was reproduced to an accuracy of 14%). Sometimes we observed a pattern that was apparently a superposition of several trains of bursts of different frequency and amplitude.

All of the illustrations given below pertain to the two most completely studied samples: No. 1, in the lower diode (initial pressure in the bcc phase $p_0 = 32.2$ atm, $T < 1$ K, hcp + bcc in the lower diode, bcc in the upper diode), and No. 2, in the upper diode ($p_0 = 30.3$ atm, hcp in the lower diode, hcp + bcc in the upper diode). It should be noted that the data in Figs. 3–6 were obtained on sample No. 1, and those in Figs. 7 and 8 were obtained on sample No. 2.

Figure 3 shows an example of the current bursts recorded in sample No. 2 at $T = 0.9$ K for voltages $U = 267$, 500, and 800 V. Depending on the sample, at voltages U less than 100–300 V the bursts were either not observed or occurred chaotically with different intervals Δt and integrated charge Q (here the average current $Q/\Delta t$ of the bursts was approximately constant, i.e., the frequent bursts were small and the rare bursts were large, as can be seen in Fig. 3a). At voltages above 300 V and up to a certain threshold $U_{\text{upper}}(T)$ a stable oscillatory regime was observed (Fig. 3b,c).

The time interval $\Delta t(T)$ between bursts ($U = \text{const}$) increased exponentially with inverse temperature (Fig. 4a) (the transit time t^* of the free charges across the interelectrode space also increased exponentially, but with a somewhat smaller activation energy; see Fig. 4b). The field dependence $\Delta t(U)$ for two different temperatures is shown in Fig. 5a.

The duration τ of a burst (full width at half maximum) could be recorded reliably for $T < 0.9$ K, i.e., when it was substantially longer than the time constant of our recording system $\tau_0 \sim 0.2$ s. The duration τ increased exponentially as the temperature decreased with an activation energy of 7–8 K and exceeded 2 s at 0.7 K (Fig. 4c). At a single temperature the values of τ were about the same for different voltages. The pulse shape of the bursts was close to triangular, so that the integrated charge Q was determined as $Q = I_m \tau$, where I_m is the pulse height.

For $T > 0.9$ K, with $\tau < \tau_0$, the burst pulses had a steep rise and an exponential fall with the instrumental time constant τ_0. In this case the charge in a burst could be determined as

$$Q = \int_0^\infty I_m \exp(-t/\tau_0)\, dt = I_m \tau_0. \tag{2}$$

The maximum charge Q varied from 10^{-12} C to 10^{-11} C in different samples (Fig. 5b), and the maximum average current $Q/\Delta t$ of the oscillatory component varied from 0.4% (Fig. 5c) to 2% of the total steady-state current. As the voltage approached the upper threshold $U_{\text{upper}}(T)$ the charge Q decreased rapidly and the bursts disappeared. The

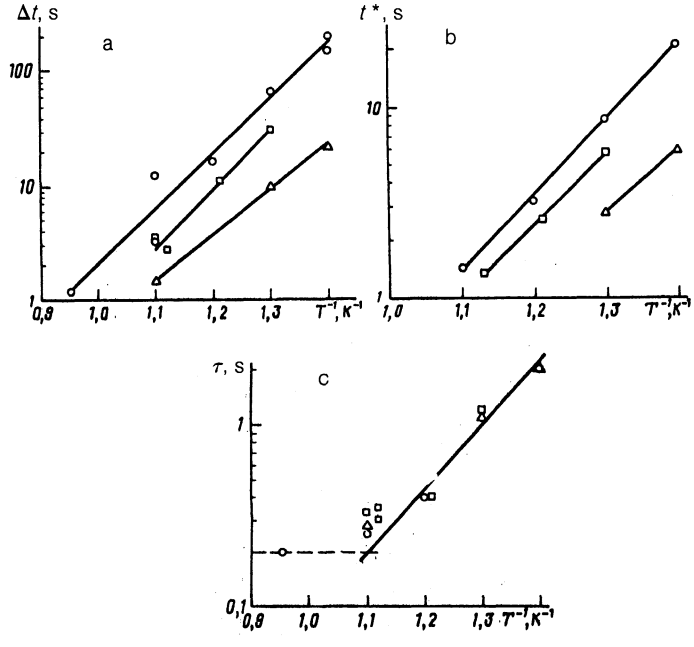

FIG. 4. Plots of Δt, t^*, and τ versus the inverse temperature in sample No. 2 at $U = 300$ V (○), 400 V (□), 600 V (△) (the solid lines are exponential approximations). a: Δt, the interval between bursts; the activation energies are 11.2 K (300 V), 12.0 K (400 V), 9.2 K (600 V). b: t^*, the transit time of the charges across the interelectrode space; the activation energies are 9.0 K (300 V), 8.5 K (400 V), and 7.5 K (600 V). c: τ, the duration of the burst (the dashed line shows the time constant of the detection system, $\tau_0 \approx 0.2$ s); the activation energy obtained from the slope of the solid line is 8.0 K.

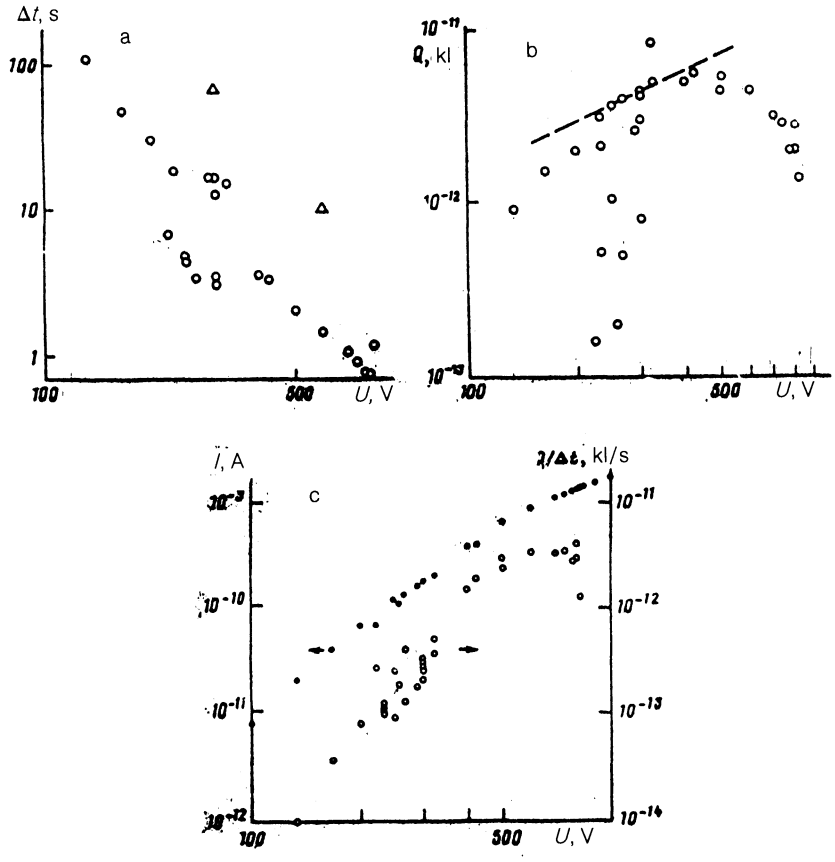

FIG. 5. Plots of Δt, Q, I, and $Q/\Delta t$ versus the voltage U in sample No. 2 at temperatures of 0.91 K (○) and 0.77 K (△). The spread of values for $U = 220$–330 V corresponds to the chaotic regime (as in Fig. 3a). a: Δt, the interval between bursts. b: Q, the integrated charge in a burst; the dashed line shows a linear dependence $Q \propto U$. c: $Q/\Delta t$, the average current in the bursts (○), and $I(U)$, the field dependence of the steady-state current (●).

value of $U_{upper}(T)$ increased with decreasing temperature.

It should be noted that when the voltage was turned on abruptly the bursts began to occur with a highly reproducible delay following the arrival of the charge front at the collector (Fig. 6). The value of the delay was of the order of the interval Δt between bursts.

New threshold effects in the appearance and disappearance of bursts were observed in weak fields. As we have said, regular oscillations of the current were observed in a bounded interval of voltages $U_{lower} - U_{upper}$ and only at temperatures below 1 K (Fig. 7). At the time of the transition through the upper threshold U_{upper} (shown by the dashed line in Fig. 7) the charge Q decreased smoothly to zero, and as the voltage U was decreased the burst either became chao-

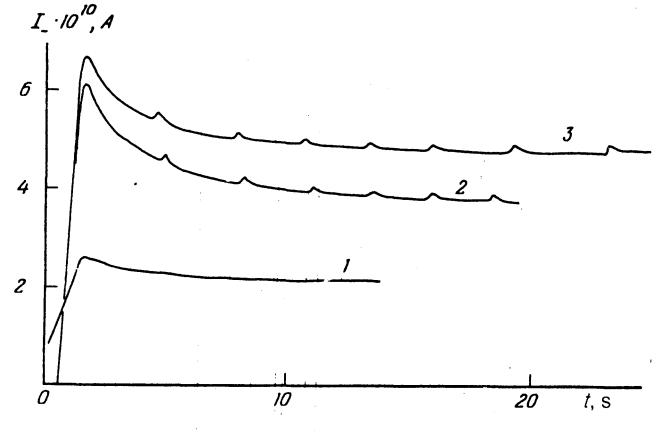

FIG. 6. Time dependence of the current of negative charges $I(t)$ when a voltage $U = -300$ V is turned on (curve 1). Curves 2 and 3 are plotted with a fivefold magnification (the zero has been shifted) to demonstrate the reproducibility of the delay of the onset of current oscillations after the voltage is turned on. Sample No. 2, $T = 0.91$ K.

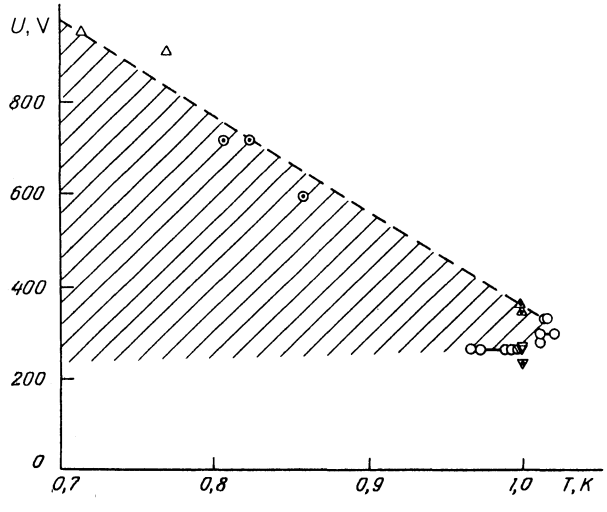

FIG. 7. The (shaded) region of voltages U and temperatures T in which regular bursts of negative current were observed. The symbol ○ denotes the boundary of this region measured for varying temperature ($U = $ const), as in Fig. 8a (the points connected by a horizontal line show the hysteresis in the appearance and disappearance of current bursts upon cooling and heating in weak fields). The symbols △ and ▽ show points obtained by varying the voltage U ($T = $ const; see Fig. 8b) about the upper and lower threshold fields, respectively. The dashed line is drawn as an aid to the eye. Sample No. 1. The data represented by the symbols with a dot inside were obtained in the first day of measurements, those represented by the empty symbols were obtained the next day.

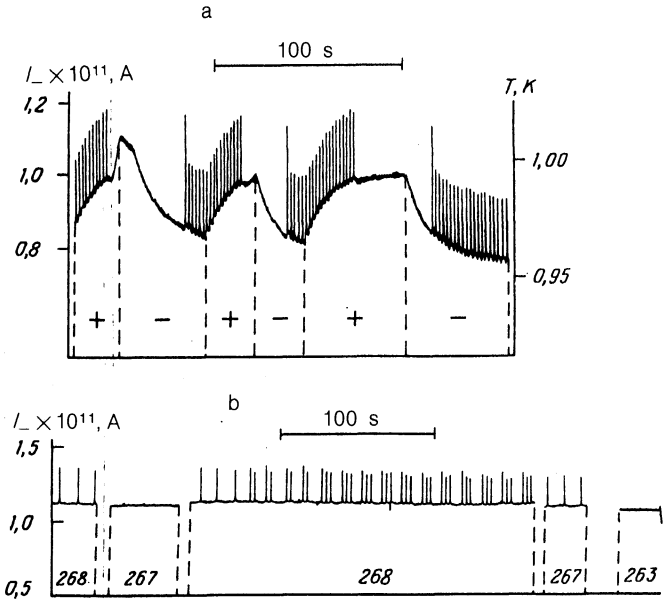

FIG. 8. Examples of the recordings of the current of negative charges $I_-(t)$ at the transition through the lower boundary of the existence region of regular bursts in sample No. 1. a: At a constant voltage $U = -267$ V during heating (+) and cooling (−); the temperature of the sample corresponding to the steady-state component of the current (the lower envelope of the curve) is indicated on the right. b: At a constant temperature $T = 1.00$ K for various values of the voltage U (the numbers under the curves).

tic (as in Fig. 3a) or vanished suddenly from a finite Q at a lower threshold voltage U_{lower}. When the voltage was again increased the bursts suddenly reappeared, with a certain hysteresis with respect to U (Fig. 8b).

Threshold behavior for the appearance and disappearance of the bursts and hysteresis in the thresholds was also observed in connection with smooth changes in temperature near 1 K. Figure 8a shows a recording of the threshold behavior of the appearance and disappearance of the bursts during thermal cycling near the minimum voltage $U = 267$ V. With increasing temperature the regular bursts suddenly vanished at $T_1 = 0.990$ K, and on subsequent cooling they suddenly reappeared, but at $T_2 = 0.967$ K. The values of T_1 and T_2 were well reproducible. On cooling, the charge of the first burst, $Q_0 = 6 \cdot 10^{-13}$ C, was noticeably larger than that of the subsequent bursts, $Q = 3.5 \cdot 10^{-13}$ C.

4. DISCUSSION OF THE RESULTS

The onset of current bursts indicates that some kind of large defects, capable of accumulating and coherently releasing a charge of up to $3 \cdot 10^7 e$, arise in two-phase hcp–bcc samples of solid helium. It was shown in Ref. 2 that because of the limitation on the value of the space charge in such electric fields, a single one-dimensional defect (a dislocation) can accumulate a charge only of the order of $10^5 e$ cm^{-1}. Therefore one must speak of a set of dislocations (a dislocation wall). Since in these experiments the bursts were observed only in two-phase samples, the possible charge traps can be located either at grain boundaries and dislocation pileups in the region where the sample is plastically deformed owing to recrystallization from the bcc to the hcp phase, or else on the interface between the bcc and hcp phases.

We are inclined toward the first interpretation, since in Ref. 2 current bursts arose in single-phase samples of solid helium after plastic deformation of the crystal caused, e.g., by melting part of it (the change in the molar volume was $\Delta V_m / V_m \sim 4\%$). During recrystallization of part of our sample from the bcc to the hcp phase the change in the molar volume was $\Delta V_m / V_m \sim 1\%$, which should also lead to plastic flow of the solid helium. Consequently, the conditions of plastic deformation in our experiment and in Ref. 2 were not too different.

In what follows we consider a certain planar defect (a dislocation wall) with an effective area S^*, located a distance l^* from the collector. As we shall see later, $(S^*)^{1/2} > l^*$ holds, and for making estimates we neglect edge effects. Solitary mobile charges are trapped by this defect, and subsequently a charged wall moves through the crystal toward the collector. The maximum charge that can be accumulated by an immobile defect of this kind at a diode voltage U is

$$Q = \varepsilon U S^* / l^*, \tag{3}$$

and, accordingly, the mechanical stress acting on the charged plane is

$$\sigma = QE/S^* = \varepsilon U^2 / 2 l^{*2}. \tag{4}$$

Depending on the temperature, we can distinguish three ranges of electric fields:

1) Weak fields (voltages much below the threshold U_{lower}), where the defect is practically immobile, and the value of the accumulated charge is described by expression (3).

2) Intermediate fields (voltages between U_{lower} and U_{upper}), in which regular bursts are observed. With increasing U the stress $\sigma \propto U^2$ increases rapidly, and in fields above a certain threshold field $E > U_{\text{lower}} / l^*$ the charged wall begins to move (flexes) toward the collector, near which it discharges and returns to its initial state. This process then repeats cyclically. With increasing voltage U the force acting on the defect becomes substantially greater than the retarding forces, and the velocity of the defect (and with it the frequency of the current oscillations) is determined more and more by the mobility of the charges themselves.

3) Strong fields (voltages above U_{upper}), in which the electric field significantly decreases the depth of the potential well of a charge at a defect and facilitates the thermally activated release of charge. Therefore the upper threshold voltage U_{upper} decreases with increasing temperature.

This idealized picture clearly pertains to a mobile dislocation wall with a well-defined contour that is pinned at the intersections of the dislocations. Then, after the lower threshold field is surpassed, one should observe strictly periodic current bursts. If different parts of the wall are pinned differently, then with increasing load (with accumulation of charge or increase in the external field) new parts come into play in the charge transport, giving rise to a train of bursts of different amplitude in weak fields (Fig. 3a, sample No. 2). Because of this, the value of the effective area S^* can change as U increases, and this is manifested in a nonlinear dependence $Q(U)$ (in Fig. 5a the dependence $Q \propto U$ is shown by the dashed line). If several mobile walls with different param-

eters are present simultaneously in the sample then a complex mixed pattern of oscillations can arise, as was in fact observed in a number of samples.

Using formulas (3) and (4) for an immobile defect (located approximately in the center of the sample, i.e., $l^* \sim 0.1$ mm), we can estimate the lower threshold stress σ_c which is sufficient to initiate motion of the defect. In Fig. 8a (sample No. 1, $T = 0.967$ K) for $U = 267$ V the first burst corresponds to a charge $Q = 6 \cdot 10^{-13}$ C, so that the effective area is $S^* \sim 3 \cdot 10^{-3}$ cm^2, and $\sigma_c \sim 3 \cdot 10^2$ dyn/cm^2. This value of σ_c is three orders of magnitude lower than the plastic flow stress in bcc solid helium at low pressures.[14-16] However, those grain boundaries with small angles of misorientation θ might move. We note that unexpectedly small values of the lower threshold stress, 80–350 dyn/cm^2, have also been observed[5] in studies of the motion of charged low-angle boundaries in alkali halide crystals at high temperatures!

Let us consider the case of intermediate fields, which corresponds to the shaded region in Fig. 7. After the voltage is turned on it is necessary first to charge the defect, since regular bursts began only after the charges had passed through the bcc phase (Fig. 6, transit time through the bcc phase $\tau^* = 1.6$ s, oscillation period $\Delta t = 2.9$ s), and it can be concluded that the defect is found in the bcc crystal (or, at least, that the bcc crystal lies between it and the source of charges), since at temperatures $T = 1$–0.7 K the mobility of the negative charges μ_- in the bcc phase (10^{-5}–10^{-7} cm^2/V·s) is three or four orders of magnitude larger than in the hcp phase. Further evidence that the defect moves in the bcc and not the hcp crystal comes from the fact that the values found for the characteristic activation energy for the decrease in the period of the bursts in intermediate fields, 8–10 K, are close to the activation energies for motion of negative charges in the bcc phase (see Fig. 4a,b), while in the hcp phase it is around 20 K (Ref. 11).

Assuming that in intermediate fields the dislocations move freely together with the moving charges, we can estimate the values of σ_c and S^* in this range of fields as well, knowing the fraction of the current that is transported by the bursts and the area S_0 of the bcc phase. In sample No. 2, according to measurements of μ_- and I_∞ (Fig. 6) and formula (1), the area S_0 equaled 0.9 cm^2, or about 90% of the area of the electrodes (for comparison, in sample No. 1 it was about 10%). The ratio of the current transported by a burst to the total steady-state current varied from 10^{-3} to $5 \cdot 10^{-3}$, depending on the voltage U (Fig. 5); consequently, $S^* \sim 10^{-3}$–$5 \cdot 10^{-3}$ cm^2. Knowing that the charge at voltages $U = 300$–400 V was $Q = 5 \cdot 10^{-12}$ C (Fig. 4), we obtain $\sigma_c \sim QU/LS^* \sim 10^2$ dyn/cm^2, which again supports the conclusion that the ultimate load σ_c is very low.

Experiments on the attenuation of ultrasound[17] imply that the main centers for pinning of dislocations in solid ^{4}He at concentrations of impurity ^{3}He above 1% are ^{3}He atoms. Hysteresis effects in the appearance and disappearance of current bursts near the lower boundary $U_{\text{lower}}(T)$ between the regions of weak and intermediate fields (Fig. 7) and the difference in the amplitudes of the first and subsequent bursts (Fig. 8a) can be attributed to a difference in the concentrations of ^{3}He atoms on moving and sessile defects. Since a rapidly moving defect does not entrain ^{3}He atoms behind it, the concentration of ^{3}He near it corresponds to the bulk value $x = 5\%$. At the same time, a sessile defect can accumulate $x_0 = x \exp(W_0/T)$ ^{3}He atoms (W_0 is the binding energy of a ^{3}He atom with the defect). The external force QE required to tear the defect away from the ^{3}He atoms is proportional to this quantity. The first burst in Fig. 8a ($E = \text{const}$) has a charge Q_0 that is 1.6 times as large as the charge Q in the subsequent bursts, when the defect has become mobile. We can estimate W_0 from the ratio of the amplitudes of the first and subsequent bursts:

$$Q_0/Q = 1{,}6 = x_0/x = \exp(W_0/T), \tag{5}$$

which gives

$$W_0 = (0{,}97\,\text{K}) \cdot \ln 1{,}6 = 0{,}46\,\text{K}. \tag{6}$$

This value is close to the value 0.3 K obtained for the binding energy of a ^{3}He atom with dislocations in hcp ^{4}He in experiments on the attenuation of ultrasound.[17]

The presence of an upper limiting temperature for the existence of current bursts in weak fields (Fig. 8a) and its decrease with increasing voltage U (Fig. 7) suggests that the ultimate load for the onset of motion of a defect in this case decreases on cooling (rather than increases, as is ordinarily the case in other materials such as NaCl; Ref. 5). This fact in principle agrees with the observations of a number of authors[15-18] that dislocations in solid helium become more mobile at $T < 1$ K, and the yield strength in bcc ^{4}He and ^{3}He is athermic or falls off with decreasing temperature.

Let us now consider the conditions necessary for observation of charge bursts in the model of a mobile charged defect:

—The applied electric field and the temperature of the sample must not be too small, so that there is sufficient time for the defect to become charged and reach the collector in a reasonable time (e.g., the transit time t^* must not be more than ten minutes, i.e., the mobility μ of the charges must be not less than 10^{-8} cm^2/V·s).

—The electric field and temperature must not be too high, so that the charges of a given sign trapped by the defect are not torn away by the field.

—The field must not be too weak, so that the force exerted on the defect exceeds the temperature-dependent limiting value necessary for tearing the defect away from the pinning centers.

The region of temperatures and voltages in which these conditions can be met depends on the relationship between the mobilities of the charges and defects and between the values of the binding energy of the charges with the defects and the critical load necessary for motion of a defect, and also on the defect concentration. Evidently these conditions are met in the shaded region in Fig. 7 for deformed samples of the bcc phase in the case of negative charges. The fact that we did not observe bursts of positive current in the same samples can be attributed to the low mobility of positive charges in the bcc phase.

CONCLUSION

In this paper we have demonstrated for the first time the possibility of observing the motion of charged macroscopic defects in ^{4}He + ^{3}He solid solutions. In weak electric fields we have detected threshold behavior in the appearance and

disappearance of quasi-periodic current oscillations due to the charging and motion of these defects as the applied field or temperature is increased or decreased. The current oscillations have been successfully described in a model based on the motion of charged low-angle grain boundaries.

We are grateful to A. V. Lokhov for assistance in the experiments and to A. J. Dahm and A. A. Levchenko for helpful discussions.

[1] S. C. Lau, A. J. Dahm, and W. A. Jeffers Jr., J. Phys. (Paris) **39**, Colloq. C6-86 (1978).
[2] B. M. Guenin and A. J. Dahm, Phys. Rev. B **23**, 1139 (1981).
[3] A. J. Dahm, in *Progress in Low Temperature Physics*, Vol. 9 (ed. by D. F. Brewer), North-Holland, Amsterdam (1985).
[4] V. S. Bobrov and M. A. Lebedkin, Fiz. Tverd. Tela (Leningrad) **31**(6), 120 (1989) [Sov. Phys. Solid State **31**, 982 (1989)].
[5] R. J. Schwensfeir and C. Elbaum, J. Phys. Chem. Solids **28**, 597 (1967).
[6] A. V. Gudenko and V. L. Tsymbalenko, Zh. Eksp. Teor. Fiz. **76**, 1399 (1979) [Sov. Phys. JETP **49**, 712 (1979)].
[7] V. B. Efimov and L. P. Mezhov-Deglin, Fiz. Nizk. Temp. **8**, 466 (1982) [Sov. J. Low Temp. Phys. **8**, 228 (1982)].
[8] F. F. Levchenko and L. P. Mezhov-Deglin, Zh. Eksp. Teor. Fiz. **86**, 2123 (1984) [Sov. Phys. JETP **59**, 1234 (1984)].
[9] A. I. Golov and L. P. Mezhov-Deglin, Proc. LT-19; Physica B **165–166**, 813 (1990).
[10] A. I. Golov and L. P. Mezhov-Deglin, Proc. LT-19; Physica B **165–166**, 811 (1990).
[11] A. I. Golov, V. B. Efimov, and L. P. Mezhov-Deglin, Zh. Eksp. Teor. Fiz. **94**(2), 198 (1988) [Sov. Phys. JETP **67**, 325 (1988)].
[12] A. I. Golov, V. B. Efimov, and L. P. Mezhov-Deglin, Pis'ma Zh. Eksp. Teor. Fiz. **40**, 293 (1984) [JETP Lett. **40**, 1080 (1984)].
[13] G. H. Vignos and H. A. Fairbank, Phys. Rev. **147**, 185 (1966).
[14] A. Sakai, Y. Nishioka, and H. Suzuki, J. Phys. Soc. Jpn. **46**, 881 (1979).
[15] D. J. Sanders, H. Kwun, A. Hikata, and C. Elbaum, J. Low Temp. Phys. **35**, 221 (1979).
[16] M. B. Manning, M. J. Moelter, and C. Elbaum, Phys. Rev. B **33**, 1634 (1986).
[17] I. Iwasa and H. Suzuki, J. Phys. Soc. Jpn. **49**, 1722 (1980).
[18] J. R. Beamish and J. P. Franck, Phys. Rev. Lett. **47**, 1736 (1981).

Translated by Steve Torstveit